GPU-Accelerated State-Averaged CASSCF Interfaced with Ab Initio Multiple Spawning Unravels the Photodynamics of Provitamin D_3

James W. Snyder Jr.,[1,2] Basile F. E. Curchod,[1,2] and Todd J. Martínez[1,2]

[1]Department of Chemistry and The PULSE Institute, Stanford University, Stanford, CA 94305
[2]SLAC National Accelerator Laboratory, Menlo Park, CA 94025

Abstract

Excited-state molecular dynamics is essential to the study of photochemical reactions, which occur under nonequilibrium conditions. However, the computational cost of such simulations has often dictated compromises between accuracy and efficiency. The need for an accurate description of both the molecular electronic structure and nuclear dynamics has historically stymied the simulation of medium- to large-size molecular systems. Here, we show how to alleviate this problem by combining *ab initio* multiple spawning (AIMS) for the nuclear dynamics and GPU-accelerated state-averaged complete active space self-consistent field (SA-CASSCF) for the electronic structure. We demonstrate the new approach by first principles SA-CASSCF/AIMS nonadiabatic dynamics simulation of photoinduced electrocyclic ring-opening in the 51-atom Provitamin D_3 molecule.
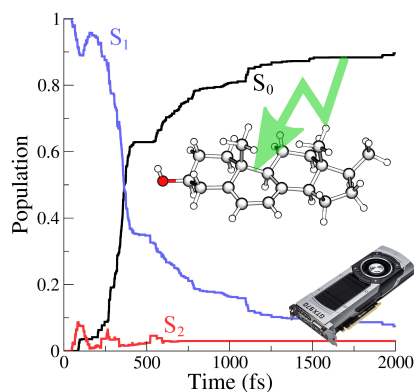
From the development of solar energy technology to enhanced fluorescent proteins, the study of light-induced processes is of great importance to modern science, yet photochemical reactions are still challenging to rationalize. Excited-state potential energy surfaces are quite complex, often exhibiting multiple avoided crossings or conical intersections (CIs) between two or more electronic states.[1-5] Furthermore, photochemical reactions occur under nonequilibrium conditions, typically on the femtosecond to picosecond timescale.[6-7] Although advances in ultrafast spectroscopy have enabled detailed studies of such reactions,[6] these experiments are not straightforward to perform and their results can be difficult to interpret. Theoretical methods provide an electronically and atomically-resolved model for photochemical processes, thus providing insight into phenomena that cannot be observed experimentally. As such, the development of theoretical methods is of great importance to the study of photochemistry.

Despite its importance, theoretical studies of photochemical processes are still quite challenging. Because vibrational relaxation occurs on the picosecond timescale, statistical methods,[8] such as transition state theory, are generally not valid. Even pathway-oriented reaction mechanisms, such as minimum energy[2] and intrinsic relaxation[9] pathways, cannot account for the nonequilibrium dynamical behavior of the system, which can be important for even a qualitative description of photochemical processes. As a result, one of the most effective theoretical methods for the study of photochemical reactions is explicit simulation of the nonadiabatic dynamics following light absorption. Unlike standard molecular dynamics, nonadiabatic dynamics does not rely on the validity of the Born-Oppenheimer approximation. It can properly treat transitions involving avoided crossings and CIs, which are ubiquitous on excited-state potential energy surfaces. An accurate excited-state dynamics would treat the nuclear degrees of freedom quantum-mechanically, as nuclear quantum effects are significant

close to CIs. However, the cost of such calculations scales exponentially with the number of degrees of freedom,[10-11] often requiring reduced dimensionality treatments which preselect a few important modes. Ab initio nonadiabatic molecular dynamics represents a compromise between efficiency and accuracy that includes surface crossing (nonadiabatic) effects while determining the required potential energy surfaces from simultaneous solution of the electronic Schrödinger equation.[12-21] Quantum mechanical effects related to surface crossing can be described either by a swarm of classical trajectories that can *hop* between electronic states – trajectory surface hopping (TSH)[22-24] – or by an expansion of the nuclear wavefunctions in terms of frozen Gaussians following classical trajectories called "trajectory basis functions" – Full Multiple Spawning (FMS)[12-13,25-27] and related methods.[19,28-30] The propagation of trajectories substantially reduces the cost of the nuclear propagation compared to grid-based solution of the time-dependent Schrödinger equation.[10-11] However, when implemented in a context where the electronic structure is solved simultaneously with the nuclear dynamics, a large number of electronic structure calculations will be required to compute electronic energies, nuclear gradients, and nonadiabatic coupling vectors between electronic states. As such, a tradeoff between efficiency and accuracy has to be found – both for the nuclear dynamics and the electronic structure – to apply *ab initio* nonadiabatic dynamics to medium to large-size molecules.

Due to its efficiency and simplicity, fewest-switches TSH, pioneered by Tully, is one of the most popular methods of nonadiabatic dynamics. Despite this popularity, TSH has some important deficiencies. TSH employs a swarm of independent classical trajectories and therefore cannot capture quantum nuclear effects such as tunneling or wavepacket interference. It also suffers from the well-known decoherence problem because trajectories on each surface are

propagated coherently over the course of an entire simulation, irrespective of the shape of the individual potential energy surfaces.[31-35] As it is not derived from first principles, TSH may converge to the wrong solution, due, in part, to the decoherence problem.[14,34] The FMS method is an alternative to TSH that is derived from first principles as an adaptive basis set expansion of the time-dependent Schrödinger equation. In a complete basis set, the FMS method is formally exact. Furthermore, it can be combined with "on the fly" electronic structure calculations, leading to the *ab initio* multiple spawning (AIMS) method. In FMS and AIMS, multiple coupled trajectories are propagated simultaneously, thus automatically accounting for decoherence of the nuclear wavepacket. Although the number of electronic structure calculations scales formally quadratically with the number of trajectory basis functions (TBFs), this cost can be significantly reduced with a judicious set of spawning constraints.[13] Moreover, by propagating a set of coupled trajectories, FMS converges more quickly than TSH.[36] In short, FMS is formally more rigorous and similarly expensive in relation to TSH.

Both TSH and AIMS can, in principle, be coupled to any electronic structure method, but linear-response time-dependent density functional theory (LR-TDDFT) has been a common choice for large molecular systems, primarily due to its weak scaling of computational effort with molecular size.[37-38] Thus, TSH coupled to LR-TDDFT has been used for a variety of applications.[39-42] More recently, AIMS was interfaced with GPU-accelerated LR-TDDFT and applied to study the photophysics of 4-(dimethylamino)benzonitrile (DMABN) (unpublished results). Despite its successes, LR-TDDFT has some well-known shortcomings that are due to practical approximations required to make the method tractable. Such problems include the inability to properly treat excited states with charge transfer,[43] double excitation,[44-45] and Rydberg character.[46] More importantly, it fails to accurately describe CIs between the ground

and excited states, which makes it unreliable for the study of reactions involving population transfer from an excited state to the ground state.[45]

An alternative to LR-TDDFT is state-averaged complete active space self-consistent field (SA-CASSCF).[47-49] SA-CASSCF does not exhibit the aforementioned problems with LR-TDDFT and is often considered the workhorse for the computational modeling of small to moderate sized photochemical systems. Due to the expense of traditional algorithms, however, SA-CASSCF has not previously been applied to systems comparable in size to those commonly treated by LR-TDDFT. Recent algorithmic developments capitalizing on sparsity in the atomic orbital basis have resulted in dramatic reductions in the computational scaling of SA-CASSCF. Combining these developments with GPU acceleration enables SA-CASSCF energy, gradient, and nonadiabatic coupling vector calculations on molecules with hundreds or even thousands of atoms.[50-51]

We present here the synthesis of GPU-accelerated SA-CASSCF and AIMS for the purpose of performing high accuracy nonadiabatic dynamics simulations on large photochemical systems. This marks a new stage in nonadiabatic dynamics, as it simultaneously improves the accuracy of the electronic structure calculation (SA-CASSCF) and the nuclear dynamics propagation (AIMS) for the excited-state dynamics of medium- to large-size molecules (compared to LR-TDDFT and TSH approaches). In this sense, it pushes the aforementioned compromise between accuracy and efficiency to a new limit. To demonstrate the computational power of our implementation, we applied AIMS coupled to SA-CASSCF to the light activated ring opening of provitamin D_3 (Pro). Details of our simulation will be presented below, but first we emphasize its size. Each of the 30 sets of initial conditions for the 51-atom Pro analog, shown pictorially in Figure 1, was propagated for up to 2 picoseconds. A total of 330 TBFs were

spawned during the course of the simulation, with each time step requiring at least one SA-CASSCF involving 249 electronic basis functions. As such, this is one of the largest fully *ab initio* nonadiabatic dynamics simulations ever performed.

The electrocyclic ring opening of Pro to form previtamin D_3 (Pre) is the light catalyzed step in the *in vivo* mammalian synthesis of vitamin D_3. Aside from its obvious biological importance, Pro is a model system for understanding how to optically control polyene chromophores, which has potential applications in nanoscience.[52] This reaction has been studied both experimentally[53-62] and theoretically.[63-64] Critical points on Pro potential energy surfaces are represented in Figure 1 (SA-3-CAS(6,4)/6-31G, see SI for details and validation of the electronic structure employed).[65-66] Upon photoexcitation in S_1, the molecule can either visit S_2 or reach the ground state (S_0) *via* CIs. Upon reaching the S_1/S_0 CI (right panel of Figure 1), the molecule can either react to form Pre in the ground state, or return to its original Pro form. In early experimental work, Jacobs, *et al.* demonstrated[54,56] that the quantum yield for the formation of Pre was 0.34 in solution.[67] More recently, Tang *et al* employed ultrafast UV-vis transient absorption spectroscopy to demonstrate that the photoconversion of Pro to Pre exhibits biexponential decay, with time constants ranging from 0.39-0.65ps and 1.06-1.81ps depending on the solvent.[59] Tapavicza *et al* comprehensively studied the photochemistry of Pro and Pre using TSH coupled to LR-TDDFT.[64] At variance with experimental results, the computed reaction rates are too fast and the population decay is not biexponential. These discrepancies may be due to some of the shortcomings of TSH and LR-TDDFT discussed previously.
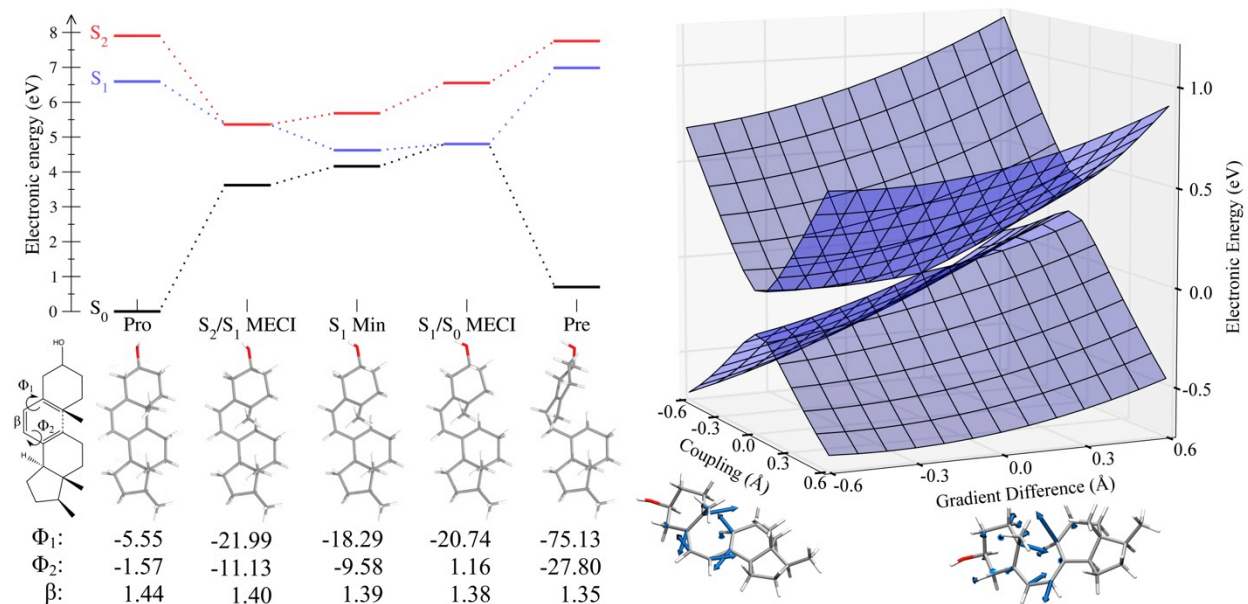
Figure 1. Left panel: critical points on the PESs of provitamin D_3 and corresponding structures. Right panel: branching space around the S_1/S_0 minimal energy conical intersection (MECI).

We performed *ab initio* nonadiabatic molecular dynamics with AIMS coupled to SA-3-CAS(6,4)/6-31G from a set of 30 initial conditions. The initial conditions were drawn from a harmonic Wigner distribution (corresponding to geometry and frequencies from PBE0/6-31G*) and propagated for up to 2 picoseconds. Every simulation was followed until effectively all of the population had reached the ground electronic state.[68] The populations of S_0, S_1, and S_2 are plotted as a function of time in Figure 2. There is a pronounced biexponential decay in the excited-state population with time constants (0.34±0.02)ps and (0.90±0.19)ps and normalized amplitudes 0.69±0.11 and 0.31±0.11 respectively. There are no experimental results corresponding to the population decay of Pro in the gas phase, but experimental work by Tang *et al* suggests that solvent has a relatively modest impact on the population decay time.[59] Our computed time constants are slightly faster than those reported in various solvents, which is expected since our simulations do not include the steric and viscous effects of the surrounding solvent. The amplitudes of each time constant are also not inconsistent with the experimental

results in nonpolar solvents of ~(0.50-0.65) and ~(0.35-0.5) for the fast and slow decay components respectively.[59] As such, our simulations are generally in good agreement with experiment, which lends credence to further analysis.
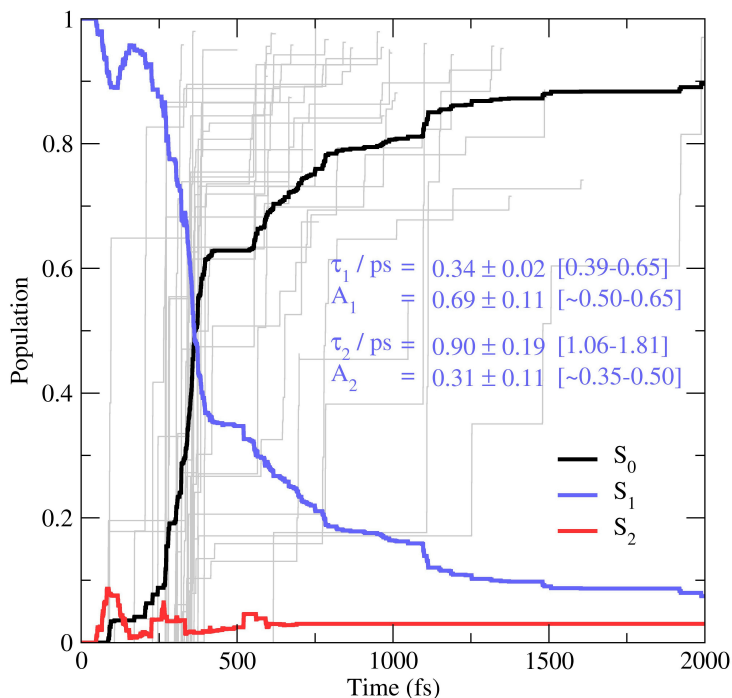

Figure 2. Population traces for the nonadiabatic decay of Pro from S_1, average over 30 initial conditions. Note the pronounced biexponential character of the excited state lifetime and ground state recovery (in agreement with experiments). Gray lines indicate the S_0 population for each individual AIMS run. Lifetimes τ_i and amplitudes A_i for each of the decaying components are indicated in the inset, with range of experimental measurements in brackets.

Aside from our simulation's good agreement with experiment, it demonstrates the importance of dynamics to understanding excited-state reactions. As evident in Figure 2, there is a small but nontrivial population in S_2 that first appears after approximately 50fs of dynamics. This demonstrates that up funneling through a CI is both possible and potentially important in photophysics, as pointed out previously.[69] Furthermore, this corroborates our prior contention that pathway-oriented reaction descriptions are deficient. By definition, a minimum energy pathway will never involve up funneling through a CI because there is always a lower energy

pathway avoiding CIs with higher lying electronic states. Excited-state systems typically gain a substantial amount of potential energy upon light absorption, which is quickly converted into kinetic energy. This excess kinetic energy can be channeled into motion that brings a molecule substantially above the minimum energy well, in this case through a CI and onto a higher potential energy surface. This phenomenon is expected to be quite general and worth exploring in further detail using nonadiabatic dynamics.
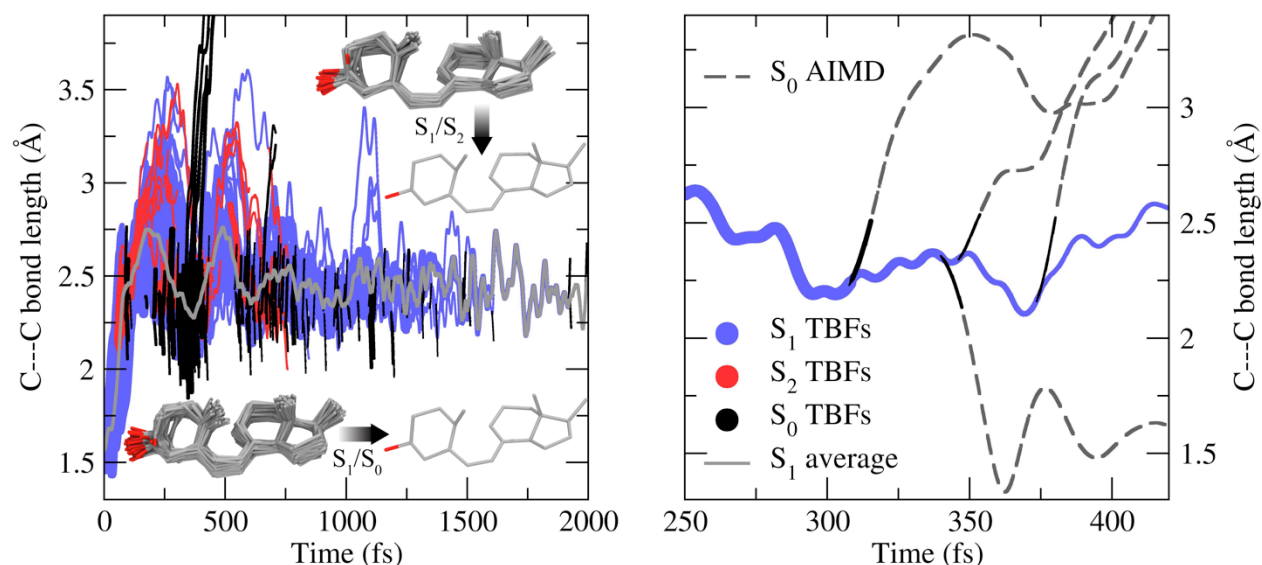
Figure 3. Projection of the AIMS TBFs population on the C—C bond opening in Pro. The thickness of the plain line indicates the population of the corresponding TBF. Left panel: Complete swarm of TBFs resulting from the AIMS dynamics. Insets compare all the S_1/S_0 (S_1/S_2) spawning geometries with the S_1/S_0 (S_1/S_2) MECI geometry (hydrogen atoms are omitted for clarity). The solid grey line is a population-weighted average of all TBFs on S_1. Right panel: zoom on a specific AIMS run, highlighting the ring-closing and ring-opening reaction when reaching S_0. Dashed gray lines represent the continuation of an AIMS TBF on S_0 with unrestricted DFT/PBE0-D3 ab initio molecular dynamics.

In addition to the electronic populations, we analyzed how the structure of provitamin D_3 changes during the course of dynamics. In the left panel of Figure 3, we plot the length of the carbon–carbon bond that breaks as a function of time for each TBF in AIMS. This bond is a structural feature clearly linked to electronic transitions (see vectors of the branching plane in Figure 1). The thickness of the line is proportional to the population carried by the corresponding

9

TBF. The right panel is the same plot for a representative trajectory over a much smaller timeframe. In the vast majority of simulations, the Pro ring breaks open within 25fs. It then mostly overshoots the region of coupling between S_0 and S_1 (sometimes spawning to S_2 in the process, red lines in Figure 3), largely because the ring opens too far prior to relaxation of the conjugated polyene bonds. After approximately 350fs, the ring contracts, reentering the S_0/S_1 coupling region, and substantial population transfer to the ground state occurs (black lines appear in Figure 3). The ring then opens more widely again and there is about a 125fs break in which no population transfer to the ground state occurs. Finally, the ring contracts again. At this point, the system is almost relaxed and the remainder of the population is transferred to the ground state more slowly over approximately 1ps. This illustrates that the biexponential character of the excited-state decay of provitamin D_3 is largely due to nonequilibrium dynamics, as opposed to a parallel or sequential reaction channels. In contrast to prior theoretical treatments,[64] we did not observe a significant difference between the reaction time of reactive (leading to ring opening) versus unreactive (preserving the ring) TBFs, which exhibit decay times of $(0.34\pm0.02)/(0.96\pm0.24)$ ps and $(0.33\pm0.02)/(0.84\pm0.15)$ ps, respectively. Importantly, the difference in the normalized amplitudes between the two classes of trajectories is not statistically significant either. This highlights the general importance of nonequilibrium dynamics to excited-state processes.

Although we do not observe parallel reaction channels that differ structurally, the nuclear momenta at the time of spawning do substantially impact the photochemical reactivity. As one can see from the right panel in Figure 3, TBFs that spawn when the ring is opening react to form Pre, while those that spawn when the ring is closing remain Pro. The origin of this phenomenon is related to the topology of the CI. As shown in Figure 1, the nonadiabatic coupling vector

corresponds to a ring opening or ring closing reaction, depending on its sign, and slopes steeply toward Pro or Pre on either side of the CI. If the molecule approaches the CI with a ring opening motion, it will react to form Pre. The opposite is true if it approaches with a ring closing motion. In a sense, this means that there are parallel reaction channels that differ, not by the molecular geometry, but rather by the nuclear momentum when entering the CI region. The topology of the CI is roughly symmetric in the direction of the coupling vector, suggesting that the quantum yield should be about 50%. In fact, the measured quantum yield for the ring opening reaction is $(51.9\pm7.9)\%$. This suggests that one might be able to change the ring-opening quantum yield by altering the S_0 and S_1 potential energy surfaces in the vicinity of the CI. It is possible that polar solvents effectively accomplish this, explaining the lower quantum yield of 0.34 in ethanol.[54,56] This is an avenue for future research.

To conclude, we would like to emphasize the following points. Modern algorithms combined with GPU acceleration enable the study of nonadiabatic dynamics for large molecular systems at the SA-CASSCF level of theory using AIMS. In the case of provitamin D_3, which is the largest system ever treated at this level of theory, the nonequilibrium dynamical behavior of the system is critical for even a qualitative understanding of the reaction mechanism. Importantly, our results are in good agreement with experimental results, validating the conclusions drawn herein. We demonstrate that the biexponential decay process observed experimentally is the result of nonequilibrium dynamics related to the opening and closing motion of the cyclohexadiene ring moiety. Our results indicate that up funneling through a CI is possible in provitamin D_3, and the reactivity of the system depends largely on its nuclear momenta, due to the topology of the potential energy surface near the CI. Further developments

11

of GPU-SA-CASSCF/AIMS will include solvent and relativistic (intersystem crossing) effects to improve the comparison between theory and experiment.[70-72]

Acknowledgments

Supporting Information Available: Details concerning electronic structure choice and validation, S_1/S_2 MECI and branching space information, SA-CASSCF orbitals and eigenvectors for the critical points. This material is available free of charge via the Internet at http://pubs.acs.org.

References

1. Bernardi, F.; Olivucci, M.; Robb, M. A., Potential Energy Surface Crossings in Organic Photochemistry. *Chem. Soc. Rev.* **1996,** *25*, 321.

2. Garavelli, M.; Bernardi, F.; Olivucci, M.; Vreven, T.; Klein, S.; Celani, P.; Robb, M. A., Potential-energy Surfaces for Ultrafast Photochemistry - Static and Dynamic Aspects. *Faraday Disc.* **1998,** *110*, 51.

3. Yarkony, D. R., Conical Intersections: The New Conventional Wisdom. *J. Phys. Chem. A* **2001,** *105*, 6277.

4. Sobolewski, A. L.; Domcke, W.; Dedonder-Lardeux, C.; Jouvet, C., Excited-state Hydrogen Detachment and Hydrogen Transfer Driven by Repulsive $(1)\pi\sigma^*$ States: A New Paradigm for Nonradiative Decay in Aromatic Biomolecules. *Phys. Chem. Chem. Phys.* **2002,** *4*, 1093.

5. Levine, B. G.; Martinez, T. J., Isomerization through Conical Intersections. *Ann. Rev. Phys. Chem.* **2007,** *58*, 613.

6. Zewail, A. H., Femtochemistry: Atomic-scale Dynamics of the Chemical Bond. *J. Phys. Chem. A* **2000,** *104*, 5660.

7. Hudock, H. R.; Levine, B. G.; Thompson, A. L.; Satzger, H.; Townsend, D.; Gador, N.; Ullrich, S.; Stolow, A.; Martinez, T. J., Ab Initio Molecular Dynamics and Time-resolved Photoelectron Spectroscopy of Electronically Excited Uracil and Thymine. *J. Phys. Chem. A* **2007,** *111*, 8500.

8. Nesbitt, D. J.; Field, R. W., Vibrational Energy Flow in Highly Excited Molecules: Role of Intramolecular Vibrational Redistribution. *J. Phys. Chem.* **1996,** *100*, 12735.

9. Garavelli, M.; Celani, P.; Fato, M.; Bearpark, M. J.; Smith, B. R.; Olivucci, M.; Robb, M. A., Relaxation paths from a conical intersection: The mechanism of product formation in the cyclohexadiene/hexatriene photochemical interconversion. *J. Phys. Chem. A* **1997,** *101*, 2023.

10. Beck, M. H.; Jackle, A.; Worth, G. A.; Meyer, H.-D., The Multiconfiguration Time-dependent Hartree (MCTDH) Method: A Highly Efficient Algorithm for Propagating Wavepackets. *Phys. Rep.* **2000,** *324*, 1.

11. Kosloff, R., Time-dependent Quantum-Mechanical Methods for Molecular Dynamics. *J. Phys. Chem.* **1988,** *92*, 2087.

12. Ben-Nun, M.; Quenneville, J.; Martinez, T. J., Ab Initio Multiple Spawning: Photochemistry from First Principles Quantum Molecular Dynamics. *J. Phys. Chem. A* **2000,** *104*, 5161.

13. Ben-Nun, M.; Martinez, T. J., Ab Initio Quantum Molecular Dynamics. *Adv. Chem. Phys.* **2002,** *121*, 439.

14. Persico, M.; Granucci, G., An Overview of Nonadiabatic Dynamics Simulations Methods, with Focus on the Direct Approach versus the Fitting of Potential Energy Surfaces. *Theo. Chem. Acc.* **2014,** *133*, 1526.

15. Barbatti, M., Nonadiabatic Dynamics with Trajectory Surface Hopping Method. *WIRES Comp. Mol. Sci.* **2011,** *1*, 620.

16. Worth, G. A.; Robb, M. A.; Lasorne, B., Solving the Time-dependent Schrodinger Equation for Nuclear Motion in One Step: Direct Dynamics of Non-adiabatic Systems. *Mol. Phys.* **2008,** *106*, 2077.

17. Martinez, T. J.; Levine, R. D., Dynamics of the Collisional Electron Transfer and Femtosecond Photodissociation of NaI on Ab Initio Electronic Energy Curves. *Chem. Phys. Lett.* **1996,** *259*, 252.

18. Vreven, T.; Bernardi, F.; Garavelli, M.; Olivucci, M.; Robb, M. A.; Schlegel, H. B., Ab Initio Photoisomerization Dynamics of a Simple Retinal Chromophore Model. *J. Amer. Chem. Soc.* **1997,** *119*, 12687.

19. Makhov, D. V.; Glover, W. J.; Martinez, T. J.; Shalashilin, D. V., Ab Initio Multiple Cloning Algorithm for Quantum Nonadiabatic Molecular Dynamics. *J. Chem. Phys.* **2014,** *141*, 054110.

20. Ben-Nun, M.; Martinez, T. J., Ab Initio Molecular Dynamics Study of cis-trans Photoisomerization in Ethylene. *Chem. Phys. Lett.* **1998,** *298*, 57.

21. Landry, B. R.; Subotnik, J. E., Quantifying the Lifetime of Triplet Energy Transfer Processes in Organic Chromophores: A Case Study of 4-(2-napthylmethyl)benzaldehyde. *J. Chem. Theo. Comp.* **2014,** *10*, 4253.

22. Tully, J. C.; Preston, R. K., Trajectory Surface Hopping Approach to Nonadiabatic Molecular Collisions - Reaction of H+ with D2. *J. Chem. Phys.* **1971,** *55*, 562.

23. Tully, J. C., Molecular Dynamics with Electronic Transitions. *J. Chem. Phys.* **1990,** *93*, 1061.

24. Drukker, K., Basics of Surface Hopping in Mixed Quantum/classical Simulations. *Journal of Computational Physics* **1999,** *153*, 225.

25. Ben-Nun, M.; Martinez, T. J., Nonadiabatic Molecular Dynamics: Validation of the Multiple Spawning Method for a Multidimensional Problem. *J. Chem. Phys.* **1998,** *108*, 7244.

26. Martinez, T. J.; Ben-Nun, M.; Ashkenazi, G., Classical/quantal Method for Multistate Dynamics: A Computational Study. *J. Chem. Phys.* **1996,** *104*, 2847.

27. Martinez, T. J.; Ben-Nun, M.; Levine, R. D., Multi-electronic State Molecular Dynamics: A Wave Function Approach with Applications. *J. Phys. Chem.* **1996,** *100*, 7884.

28. Shalashilin, D. V.; Burghardt, I., Gaussian-based Techniques for Quantum Propagation from the Time-dependent Variational Principle: Formulation in Terms of Trajectories of Coupled Classical and Quantum Variables. *J. Chem. Phys.* **2008,** *129*, 084104.

29. Shalashilin, D. V.; Child, M. S., The Phase Space CCS Approach to Quantum and Semiclassical Molecular Dynamics for High-dimensional Systems. *Chem. Phys.* **2004,** *304*, 103.

30. Worth, G. A.; Robb, M. A.; Burghardt, I., A Novel Algorithm for Non-adiabatic Direct Dynamics Using Variational Gaussian Wavepackets. *Faraday Disc.* **2004,** *127*, 307.

31. Thachuk, M.; Ivanov, M. Y.; Wardlaw, D. M., A Semiclassical Approach to Intense-field Above-threshold Dissociation in the Long Wavelength Limit. II. Conservation Principles and Coherence in Surface Hopping. *J. Chem. Phys.* **1998,** *109*, 5747.

32. Fang, J. Y.; Hammes-Schiffer, S., Improvement of the Internal Consistency in Trajectory Surface Hopping. *J. Phys. Chem. A* **1999,** *103*, 9399.

33. Granucci, G.; Persico, M., Critical Appraisal of the Fewest Switches Algorithm for Surface Hopping. *J. Chem. Phys.* **2007,** *126*, 134114.

34. Subotnik, J. E.; Shenvi, N., Decoherence and Surface Hopping: When Can Averaging Over Initial Conditions Help Capture the Effects of Wave Packet Separation? *J. Chem. Phys.* **2011,** *134*, 244114.

35. Bittner, E. R.; Rossky, P. J., Quantum Decoherence in Mixed Quantum-classical Systems: Nonadiabatic Processes. *J. Chem. Phys.* **1995,** *103*, 8130.

36. Toniolo, A.; Ciminelli, C.; Persico, M.; Martinez, T. J., Simulation of the Photodynamics of Azobenzene on its First Excited State: Comparison of Full Multiple Spawning and Surface Hopping Treatments. *J. Chem. Phys.* **2005,** *123*, 234308.

37. Runge, E.; Gross, E. K. U., Density-Functional Theory for Time-Dependent Systems. *Phys. Rev. Lett.* **1984,** *52*, 997.

38. Casida, M. E., Time-Dependent Density Functional Response Theory for Molecules. *Recent Adv. Comput. Chem.* **1995,** *1*, 155.

39. Tapavicza, E.; Tavernelli, I.; Rothlisberger, U., Trajectory Surface Hopping within Linear Response Time-dependent Density-functional Theory. *Phys. Rev. Lett.* **2007,** *98*, 023001.

40. Mitric, R.; Werner, U.; Bonacic-Koutecky, V., Nonadiabatic Dynamics and Simulation of Time Resolved Photoelectron Spectra within Time-dependent Density Functional Theory: Ultrafast Photoswitching in Benzylideneaniline. *J. Chem. Phys.* **2008,** *129*, 164118.

41. Curchod, B. F. E.; Rothlisberger, U.; Tavernelli, I., Trajectory-Based Nonadiabatic Dynamics with Time-Dependent Density Functional Theory. *Chemphyschem* **2013,** *14*, 1314.

42. Barbatti, M.; Crespo-Otero, R., Surface Hopping Dynamics with DFT Excited States. In *Density-Functional Methods for Excited States*, Ferré, N.; Filatov, M.; Huix-Rotllant, M., Eds. Springer: 2016; pp 415.

43. Dreuw, A.; Weisman, J. L.; Head-Gordon, M., Long-range Charge-transfer Excited States in Time-dependent Density Functional Theory Require Non-local Exchange. *J. Chem. Phys.* **2003,** *119*, 2943.

44. Maitra, N. T.; Zhang, F.; Cave, R. J.; Burke, K., Double Excitations within Time-dependent Density Functional Theory Linear Response. *J. Chem. Phys.* **2004,** *120*, 5932.

45. Levine, B. G.; Ko, C.; Quenneville, J.; Martinez, T. J., Conical Intersections and Double Excitations in Time-dependent Density Functional Theory. *Mol. Phys.* **2006,** *104*, 1039.

46. Cheng, C. L.; Wu, Q.; Van Voorhis, T., Rydberg Energies using Excited State Density Functional Theory. *J. Chem. Phys.* **2008,** *129*, 124112.

47. Roos, B. O.; Taylor, P. R.; Siegbahn, P. E. M., A Complete Active Space SCF Method (CASSCF) Using a Density-Matrix Formulated Super-CI Approach. *Chem. Phys.* **1980,** *48*, 157.

48. Diffenderfer, R. N.; Yarkony, D. R., Use of the State-Averaged MCSCF Procedure - Application to Radiative Transitions in MgO. *J. Phys. Chem.* **1982,** *86*, 5098.

49. Schmidt, M. W.; Gordon, M. S., The Construction and Interpretation of MCSCF Wavefunctions. *Ann. Rev. Phys. Chem.* **1998,** *49*, 233.

50. Hohenstein, E. G.; Luehr, N.; Ufimtsev, I. S.; Martinez, T. J., An Atomic Orbital-based Formulation of the Complete Active Space Self-consistent Field Method on Graphical Processing Units. *J. Chem. Phys.* **2015,** *142*, 154107.

51. Snyder Jr, J. W.; Hohenstein, E. G.; Luehr, N.; Martinez, T. J., An Atomic Orbital-based Formulation of Analytical Gradients and Nonadiabatic Coupling Vector Elements for the State-averaged Complete Active Space Self-consistent Field Method on Graphical Processing Units. *J. Chem. Phys.* **2015,** *143*, 154107.

52. Rangel, N. L.; Williams, K. S.; Seminario, J. M., Light-Activated Molecular Conductivity in the Photoreactions of Vitamin D-3. *J. Phys. Chem. A* **2009,** *113*, 6740.

53. Havinga, E.; Dekock, R. J.; Rappoldt, M. P., The Photochemical Interconversions of Provitamin-D, Lumisterol, Previtamin-D and Tachysterol. *Tetrahedron* **1960,** *11*, 276.

54. Jacobs, H. J. C.; Gielen, J. W. J.; Havinga, E., Effects of Wavelength and Conformation on the Photochemistry of Vitamin-D and Related Conjugated Trienes. *Tetrahedron Lett.* **1981,** *22*, 4013.

55. Dauben, W. G.; Phillips, R. B., Effects of Wavelength on the Photochemistry of Provitamin-D3. *J. Amer. Chem. Soc.* **1982,** *104*, 5780.

56. Jacobs, H. J. C., Photochemistry of Conjugated Trienes: Vitamin D Revisited. *Pure Appl. Chem.* **1995,** *67*, 63.

57. Fuss, W.; Hofer, T.; Hering, P.; Kompa, K. L.; Lochbrunner, S.; Schikarski, T.; Schmid, W. E., Ring Opening in the Dehydrocholesterol Previtamin D System Studied by Ultrafast Spectroscopy. *J. Phys. Chem.* **1996,** *100*, 921.

58. Anderson, N. A.; Shiang, J. J.; Sension, R. J., Subpicosecond Ring Opening of 7-dehydrocholesterol Studied by Ultrafast Spectroscopy. *J. Phys. Chem. A* **1999,** *103*, 10730.

59. Tang, K. C.; Rury, A.; Orozco, M. B.; Egendorf, J.; Spears, K. G.; Sension, R. J., Ultrafast Electrocyclic Ring Opening of 7-dehydrocholesterol in Solution: The Influence of Solvent on Excited State Dynamics. *J. Chem. Phys.* **2011,** *134*, 104503.

60. Meyer-Ilse, J.; Akimov, D.; Dietzek, B., Ultrafast Circular Dichroism Study of the Ring Opening of 7-Dehydrocholesterol. *J. Phys. Chem. Lett.* **2012,** *3*, 182.

61. Arruda, B. C.; Peng, J.; Smith, B.; Spears, K. G.; Sension, R. J., Photochemical Ring-Opening and Ground State Relaxation in alpha-Terpinene with Comparison to Provitamin D-3. *J. Phys. Chem. B* **2013,** *117*, 4696.

62. Arruda, B. C.; Sension, R. J., Ultrafast Polyene Dynamics: the Ring Opening of 1,3-Cyclohexadiene Derivatives. *Phys. Chem. Chem. Phys.* **2014,** *16*, 4439.

63. Bernardi, F.; Olivucci, M.; Ragazos, I. N.; Robb, M. A., A New Mechanistic Scenario for the Photochemical Transformation of Ergosterol - An MCSCF and MM-VB Study. *J. Amer. Chem. Soc.* **1992,** *114*, 8211.

64. Tapavicza, E.; Meyer, A. M.; Furche, F., Unravelling the Details of Vitamin D Photosynthesis by Non-adiabatic Molecular Dynamics Simulations. *Phys. Chem. Chem. Phys.* **2011,** *13*, 20986.

65. Tao, H. L. First Principles Molecular Dynamics and Control of Photochemical Reactions. PhD Thesis, Stanford University, 2011.

66. Kim, J.; Tao, H. L.; White, J. L.; Petrovic, V. S.; Martinez, T. J.; Bucksbaum, P. H., Control of 1,3-Cyclohexadiene Photoisomerization Using Light-Induced Conical Intersections. *J. Phys. Chem. A* **2012,** *116*, 2758.

67. Unfortunately, it is unclear whether the solvent used in these experiments was ethanol or heptane.

68. All trajectory basis functions remaining on the excited states had populations less than 0.05, which was the population threshold that must be exceeded to spawn new basis functions.

69. Martinez, T. J., Ab Initio Molecular Dynamics Around a Conical Intersection: Li(2p)+H2. *Chem. Phys. Lett.* **1997,** *272*, 139.

70. Virshup, A. M.; Punwong, C.; Pogorelov, T. V.; Lindquist, B. A.; Ko, C.; Martinez, T. J., Photodynamics in Complex Environments: Ab Initio Multiple Spawning Quantum Mechanical/Molecular Mechanical Dynamics. *J. Phys. Chem. B* **2009,** *113*, 3280.

71. Curchod, B. F. E.; Rauer, C.; Marquetand, P.; Gonzalez, L.; Martinez, T. J., GAIMS - Generalized Ab Initio Multiple Spawning for Both Internal Conversion and Intersystem Crossing Processes. *J. Chem. Phys.* **2016,** *144*, 101102.

72. Fedorov, D. A.; Pruitt, S. R.; Kelpert, K.; Gordon, M. S.; Varganov, S. A., Ab Initio Multiple Spawning Method for Intersystem Crossing Dynamics: Spin-Forbidden Transitions between 3B1 and 1A1 States of GeH2. *J. Phys. Chem. A* **2016,** *120*, 2911.